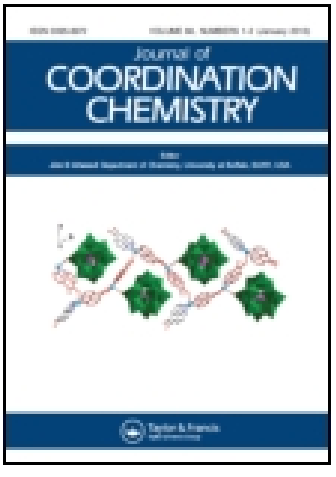

Journal of Coordination Chemistry
Publication details, including instructions for authors and subscription information:
http://www.tandfonline.com/loi/gcoo20

Metal complexes of indole-3-acetic acid: synthesis, crystal structures, and Pb^{2+} chemosensing by cation-exchange reaction

Xiangyu Zhang[a], Xuling Xue[a], Shuzi Liu[a], Min Yu[a], Hong Xu[a] & Shuangquan Zang[a]

[a] The College of Chemistry and Molecular Engineering, Zhengzhou University, Zhengzhou, PR China

Accepted author version posted online: 17 Sep 2014.Published online: 25 Sep 2014.

Journal of Coordination Chemistry, 2014
Vol. 67, No. 19, 3188–3201, http://dx.doi.org/10.1080/00958972.2014.960404

Metal complexes of indole-3-acetic acid: synthesis, crystal structures, and Pb^{2+} chemosensing by cation-exchange reaction

XIANGYU ZHANG, XULING XUE, SHUZI LIU, MIN YU, HONG XU* and SHUANGQUAN ZANG

The College of Chemistry and Molecular Engineering, Zhengzhou University, Zhengzhou, PR China

(*Received 14 January 2014; accepted 24 July 2014*)

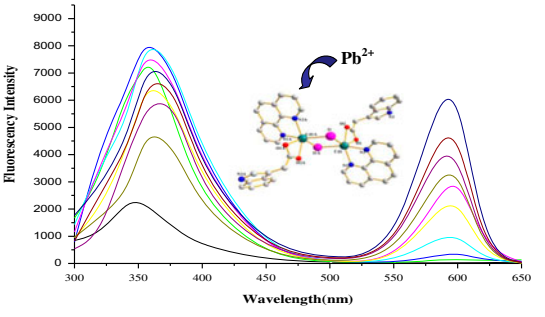

Binuclear complexes $[Cu_2(IA)_4(DMSO)_2]\cdot CH_3OH$ (**1**), $[Cd_2(IA)_2(phen)_2I_2]$ (**2**) and 1-D $\{[Pb_2(IA)_4]\cdot CH_3OH\}_n$ (**3**) (IAH = indole-3-acetic acid, phen = 1,10-phenanthroline) have been prepared and characterized by single crystal X-ray diffraction. The three complexes show strong fluorescence emissions in mixed DMF/H_2O solvent. **2** showed highly sensitive and selective sensing function to Pb^{2+} ion.

Two binuclear complexes $[Cu_2(IA)_4(DMSO)_2]\cdot CH_3OH$ (**1**), $[Cd_2(IA)_2(phen)_2I_2]$ (**2**), and one 1-D $\{[Pb_2(IA)_4]\cdot CH_3OH\}_n$ (**3**) (IAH = indole-3-acetic acid, phen = 1,10-phenanthroline) have been prepared and characterized by single crystal X-ray diffraction. Both **1** and **2** are binuclear wherein the central Cu ions are bridged by IA in **1**, while Cd ions are bridged by I^- in **2**. Complex **3** has a 1-D chain structure based on secondary building units (SBUs) of $[Pb_2(IA)_4]$. The three complexes show strong fluorescence emissions, and chemosensor behaviors for metal cations are investigated in mixed DMF/H_2O (1 : 9 v/v) solvent. The results reveal that **2** shows effective sensing to Pb^{2+}. The mechanism of the detection to Pb^{2+} can be attributed to cation-exchange reaction between cadmium and lead ions.

Keywords: Crystal structure; Indole-3-acetic acid; Cation recognition; Fluorescence

*Corresponding author. Email: xuhong@zzu.edu.cn

1. Introduction

Metal–organic complexes or metal–organic frameworks (MOFs) have emerged as a new family of sensors based on the metal-ion-induced changes in fluorescence due to simplicity and high detection limit of fluorescence [1]. Coordination or exchange of a metal ion can cause an enhancement of the fluorescence emission or a quenching of the fluorescence and both effects can be coupled with a red or blue shift of the emission band. For example, the Ln–Mn-based frameworks $[Eu(PDA)_3Mn_{1.5}(H_2O)_3]_3{\cdot}3.25H_2O$ and $[Tb(PDA)_3Mn_{1.5}(H_2O)_3]_3{\cdot}3.25H_2O$ (PDA = pyridine-2,6-dicarboxylic acid) display a significant increase in fluorescence intensity upon addition of Zn^{2+} [2]. The emission intensities of 3-D lanthanide nanoporous coordination polymers $\{[La_2(PDA)_3(H_2O)_4]{\cdot}H_2O\}_\infty$ and $\{[Pr_2(PDA)_3(H_2O)_3]{\cdot}H_2O\}_\infty$ can also be enhanced with enhancement of Cd^{2+} concentration [3]. Furthermore, metal–organic complexes of fluorescent probes for metals usually can be supported through the crystal structures of the final products, which can explain the binding mode between the chemosensor molecule and the detected metal ions [4]. The fluorescence properties can be tuned through the exchange of metal ions or organic cations within anionic MOFs, which could provide another possible route to probe cations.

Sensitive detections of toxic metals including mercury and lead are becoming increasingly important because they can accumulate in living organisms and lead to dysfunction in nervous, circulatory, and immune systems [5]. Thus, it is important to make progress to provide inexpensive and real-time monitoring methods for detection of trace amounts of mercury and lead in the environment [6]. Since Czarnik and coworkers reported the first examples of fluorescent chemosensors for Pb^{2+} in 1996 [7], many sensitive and selective chromogenic reagents, such as small molecules, calixarene, peptide, and polymers, have been developed for Pb^{2+} detection [5(b)]. However, metal–organic complexes as Pb^{2+} luminescent chemosensors are rare [1(g)] though this class represents a new kind of important luminescence for sensors.

In our previous study, we reported two zinc complexes $[Zn(IA)_2(phen)]$ and $[Zn(IA)_2(4,4'\text{-bipy})]_n{\cdot}C_2H_5OH$ based on indole-3-acetic acid (IAH), both of which exhibit fluorescence quenching when Hg^{2+} ions are present [8]. By ICP, EDS, and SEM experiments, we revealed that zinc ions in both complexes can be exchanged by toxic mercury ions. As part of our ongoing study of metal complexes based on indole-3-acetic acid, herein we report three complexes $[Cu_2(IA)_4(DMSO)_2]{\cdot}CH_3OH$ (**1**), $[Cd_2(IA)_2(phen)_2I_2]$ (**2**), and $\{[Pb_2(IA)_4]{\cdot}CH_3OH\}_n$ (**3**) (IAH = indole-3-acetic acid, phen = 1,10-phenanthroline), and discovered **2** showed effective sensing to Pb^{2+}.

2. Experimental section

2.1. *Materials and physical measurements*

IAH, phen, and solvents were of reagent quality and were obtained from commercial sources without purification. IR data were recorded on a BRUKER TENSOR 27 spectrophotometer with KBr pellets from 400 to 4000 cm^{-1}. Elemental analyses (C, H, and N) were carried out on a FLASH EA 1112 elemental analyzer. The luminescence spectra were measured on solution samples at room temperature using a model F-4500 HITACHI Fluorescence Spectrophotometer. ^1H NMR spectra were recorded on a Bruker DPX 400 instrument using DMSO-d_6 as solvent and TMS as the internal standard.

2.2. *Synthesis of complexes*

2.2.1. Synthesis of 1. To a stirred methanol solution (5 dm^3) of IAH (3.5 mg, 0.02 mM) which was adjusted to pH 7.5 using 0.01 M dm^{-3} NaOH, a methanol solution (5 dm^3) containing $CuCl_2$ (1.3 mg, 0.1 mM) was added drop-wise at room temperature. The mixture was stirred slowly for 30 min and two drops of DMSO was then added to the mixture. After standing 2 h quietly, dark-green cube crystals suitable for X-ray analysis were obtained. Yield is 87%. Anal. Calcd for $Cu_2C_{45}H_{48}O_{11}N_4S_2$(1012.04): Found C, 53.66; N, 5.61; H, 4.80; Calcd: C, 53.40; N, 5.54; H, 4.78. IR (KBr, cm^{-1}): 3272(m), 1556(s), 1438 (m), 1377(m), 1270(m), 932(w), 838(s), 745(m), 653(w). ^{1}H NMR (400 MHz, DMSO-d_6): 10.37 [1H, s, –NH], 7.12–5.43 [5H, –C6H4, –C=CH]. Because the paramagnetic Cu^{2+} presents complications in nuclear magnetic resonance, it is difficult to obtain NMR spectra.

2.2.2. Synthesis of 2. A mixture of IAH (3.5 mg, 0.02 mM) and NaOH (8.0 mg, 0.02 mM) in MeOH (5 dm^3) was stirred for 1 h. A solution of CdI_2 (3.7 mg, 0.01 mM) in MeOH (5 dm^3) was added to the above solution. The mixture was stirred quickly for 30 min. A methanol solution (3 dm^3) of phen (4.0 mg, 0.02 mM) was then added dropwise to the mixture. The solution was filtered and placed in a light-resistant environment quietly. Two weeks later, pale-yellow block crystals were generated at room temperature. Yield is 56%. Anal. Calcd for $C_{44}H_{32}Cd_2I_2N_6O_4$(1187.39): Found C, 53.71; N, 5.58; H, 4.72. Calcd: C, 53.40; N, 5.54; H, 4.78. IR (KBr, cm^{-1}): 3196(m), 1606(s), 1468(m), 1402(m), 1224(m), 959(w), 823(m), 719(w), 623(w). ^{1}H NMR (400 MHz, DMSO-d_6): δ 10.72 [1H, s, –NH], 9.09–7.98 [4H, phen], 7.46–6.86 [5H, –C6H4, –C=CH], 3.55 [2H, s,–CH2].

2.2.3. Synthesis of 3. A mixture of IAH (35.0 mg, 0.02 mM) and $Pb(OAc)_2$ (37.9 mg, 0.1 mM) in 10 mL MeOH was stirred quickly for 30 min, and then was adjusted to pH 7.0 using 0.01 M dm^{-3} NaOH. After stirring for 3 h, the white deposit was filtered. To the filtrate was added 2 mL EtOH and it was placed in a light-resistant environment quietly. Next day, colorless block crystals were generated at room temperature. Yield is 11%. Anal. Calcd for $C_{41}H_{36}N_4O_9Pb_2$ (1143.13): Found C, 43.17; N,4.97; H, 3.12. Calcd: C, 43.08; N,4.90; H, 3.17. IR (KBr, cm^{-1}): 3327 (m), 1623(s), 1541(m), 1487(m), 1237(m), 972(w), 870(s), 754(m), 672(w). ^{1}H NMR (400 MHz, DMSO-d_6): 10.78 [1H, s, –NH], 7.57–6.93 [5H, –C6H4, –C=CH], 3.35 [2H, s, –CH2]. The three complexes are insoluble in water and in common organic solvents like methanol and petroleum ether except for DMF and DMSO. Thus, all relevant solutions were prepared using DMF-containing solvent.

2.3. *Determination and refinement of the structures*

The data for **1**, **2**, and **3** were collected on a Rigaku Saturn 724 detector with graphite-monochromated Mo-Ka radiation (λ = 0.71073 Å). Single crystals suitable for X-ray diffraction were selected and mounted on a glass fiber. The data were collected at a temperature of 293 K and corrected for Lorentz-polarization effects. The structures were solved by direct methods and expanded using Fourier techniques. The nonhydrogen atoms were refined anisotropically. Hydrogens were included but not refined. The final cycle of full-matrix least-squares refinement was based on observed reflections and variable parameters. All calculations were performed using the *SHELX* 97 Crystallographic software package [9].

Table 1. Crystal data and structural refinement of **1**, **2** and **3**.

Complexes	**1**	**2**	**3**
Formula	$C_{45}H_{48}Cu_2N_4O_{11}S_2$	$C_{22}H_{16}CdIN_3O_2$	$C_{41}H_{36}N_4O_9Pb_2$
Formula weight	1012.07	593.68	1143.12
Crystal system	Orthorhombic	Monoclinic	Triclinic
Space group	*Pca2₁*	*P2₁/n*	*P-1*
a (Å)	19.302(4)	10.298(2)	11.982(2)
b (Å)	12.398(3)	18.607(4)	12.646(3)
c (Å)	18.883(4)	10.887(2)	13.677(3)
α (°)	90	90	78.30(3)
β (°)	90	102.32(3)	74.10(3)
γ (°)	90	90	79.92(3)°
V (Å^3)	4518.7(16)	2038.1(7)	1935.9(7)
Z	4	4	2
D_{Calcd} (g cm^{-3})	1.488	1.935	1.961
μ (mm^{-1})	1.098	2.610	8.747
Reflns collected	43,338	26,799	19,127
Unique reflns	7881	5490	6631
R_{int}	0.0667	0.0494	0.1050
Data/Restraints/Parameters	7177/1/574	4996/0/266	5054/13/507
GOF	1.241	1.196	1.062
$R_1[I > 2\sigma(I)]$	0.0739	0.0642	0.0790
$wR_2[I > 2\sigma(I)]$	0.1897	0.1259	0.2180

[a]$R_1 = [|F_0| - |F_c|]/|F_0|$.
[b]$wR_2 = [w(F_0^2 - F_c^2)^2]/[w(F_0^2)^2]^{1/2}$.

Crystallographic parameters, and structural refinement for **1**, **2**, and **3** are summarized in table 1. Selected bond lengths and angles of the three complexes are listed in table 2.

2.4. *Selective activities of 1, 2 and 3*

The standard water solutions of metal ions with the concentration of 1.0×10^{-5} M dm^{-3} were prepared from chloride salts of Na^+, K^+, Mg^{2+}, Ca^{2+}, Cr^{3+}, Mn^{2+}, Fe^{3+}, Co^{2+}, Ni^{2+}, Cu^{2+}, Cd^{2+} and Hg^{2+}, and nitrate of Ag^+ and Pb^{2+}, respectively. It should be mentioned that the chloride salts of Ag^+ and Pb^{2+} are not soluble in water, so we substituted them with nitrates. The standard solutions of Pb^{2+} at different concentrations were obtained by serial dilution of 1.0×10^{-5} M dm^{-3} $Pb(NO_3)_2$ solution.

It should be mentioned that the three complexes are insoluble in water and in common organic solvents like methanol and petroleum ether except for DMF and DMSO. So, the 1.0×10^{-5} M dm^{-3} stock solution of **1**, **2**, or **3** was prepared by dissolving them in DMF and then diluting in water. The ratio of DMF and H_2O is 1 : 9 (v/v). The aforementioned solutions of Pb^{2+}, **1**, **2**, and **3** stock solution were titrated in a 1/1 (v/v) ratio for subsequent fluorescence measurement. The solution samples were measured in 1.00 cm quartz cell. Furthermore, we investigated the influence of anions on the fluorescence of **1**, **2**, and **3**. The experiment results revealed that the PNO_3^- and Cl^- did not influence the fluorescence.

3. Results and discussion

3.1. *Description of the crystal structures*

3.1.1. Crystal structure of 1. The single crystal X-ray diffraction analysis has revealed that **1** crystallizes in the orthorhombic system, space group *Pca2₁*. The structure of **1** with

Table 2. Selected bond lengths (Å) and angles (°) for **1**, **2** and **3**.

Complex **1**			
Cu1–O6	1.965(5)	Cu1–O8	1.995(5)
Cu1–O1	1.970(5)	Cu1–O9	2.153(6)
Cu1–O4	1.983(5)	Cu1–Cu2	2.6129(11)
Cu2–O5	1.982(5)	Cu2–O3	1.958(5)
Cu2–O2	1.954(5)	Cu2–O7	1.962(5)
Cu2–O10	2.168(6)	O6–Cu1–O1	168.3(2)
O6–Cu1–O4	89.8(2)	O1–Cu1–O4	91.1(2)
O6–Cu1–O8	88.3(2)	O1–Cu1–O8	88.5(2)
O4–Cu1–O8	168.8(2)	O6–Cu1–O9	92.5(2)
O1–Cu1–O9	98.9(2)	O4–Cu1–O9	97.1(2)
O8–Cu1–O9	94.0(2)	O6–Cu1–Cu2	84.70(15)
O1–Cu1–Cu2	83.86(15)	O4–Cu1–Cu2	82.29(15)
O8–Cu1–Cu2	86.58(16)	O9–Cu1–Cu2	177.16(16)
O2–Cu2–O3	90.2(2)	O2–Cu2–O5	168.9(2)
O3–Cu2–O5	89.0(2)	O7–Cu2–O5	89.3(2)
O2–Cu2–O10	92.8(2)	O3–Cu2–O10	94.4(2)
O7–Cu2–O10	98.0(2)	O5–Cu2–O10	98.2(2)
O2–Cu2–Cu1	84.76(15)	O3–Cu2–Cu1	86.19(16)
O7–Cu2–Cu1	81.43(16)	O5–Cu2–Cu1	84.16(16)
O10–Cu2–Cu1	177.53(18)		
Complex **2**			
Cd1–O1	2.491(5)	Cd1–O2	2.288(4)
Cd1–N1	2.321(5)	Cd1–N2	2.335(5)
Cd1–I1	2.9136(8)		
O2–Cd1–N1	142.07(16)	O2–Cd1–N2	102.59(18)
N1–Cd1–N2	72.06(18)	O2–Cd1–O1	53.95(15)
N1–Cd1–O1	88.28(15)	N2–Cd1–O1	91.81(18)
O2–Cd1–I1A	89.36(11)	N1–Cd1–I1A	127.44(11)
N2–Cd1–I1A	90.37(15)	O1–Cd1–I1A	142.77(11)
O2–Cd1–I1	91.43(12)	N1–Cd1–I1	94.94(12)
N2–Cd1–I1	165.62(13)	N2–Cd1–I1	165.62(13)
O1–Cd1–I1	93.96(12)	I1A–Cd1–I1	92.96(3)
Complex **3**			
Pb1–O1	2.617(9)	Pb1–O2	2.417(8)
Pb1–O3	2.653(9)	Pb1–O4	2.378(8)
Pb1–O7	2.658(9)	Pb2–O3	2.669(8)
Pb2–O5	2.470(9)	Pb2–O6	2.636(8)
Pb2–O7	2.505(10)	Pb2–O8	2.444(8)
O4–Pb1–O2	86.8(3)	O4–Pb1–O2	82.7(3)
O2–Pb1–O2	65.6(3)	O4–Pb1–O1	80.2(3)
O2–Pb1–O1	50.9(3)	O2–Pb1–O1	114.6(3)
O4–Pb1–O3	52.2(2)	O2–Pb1–O3	121.6(3)
O2–Pb1–O3	130.8(3)	O1–Pb1–O3	79.5(3)
O4–Pb1–O7	115.5(3)	O2–Pb1–O7	112.6(3)
O2–Pb1–O7	161.8(3)	O1–Pb1–O7	70.5(3)
O3–Pb1–O7	66.5(3)	O8–Pb2–O5	79.4(3)
O6–Pb2–O3	166.9(3)	O8–Pb2–O7	51.8(3)
O5–Pb2–O7	102.3(3)	O8–Pb2–O6	72.8(3)
O5–Pb2–O6	51.9(3)	O7–Pb2–O6	123.5(3)
O8–Pb2–O6	72.7(3)	O5–Pb2–O6	116.4(3)
O7–Pb2–O6	102.9(3)	O6–Pb2–O6	65.4(3)
O8–Pb2–O3	106.7(3)	O5–Pb2–O3	75.8(3)
O7–Pb2–O3	68.4(3)	O6–Pb2–O3	127.3(3)

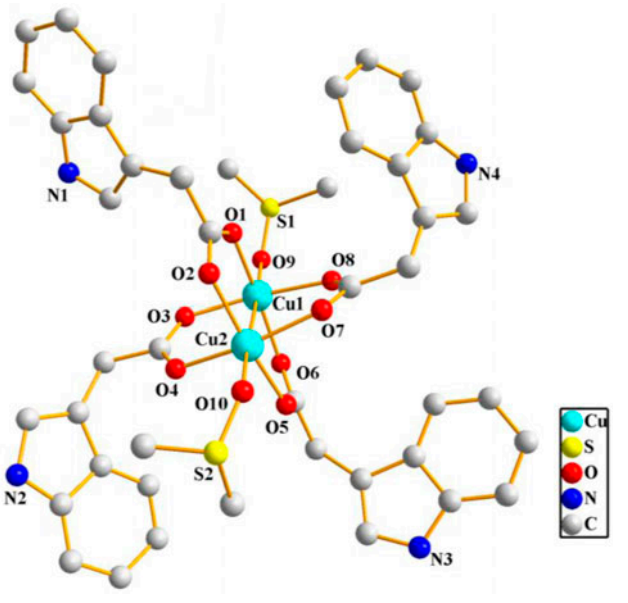

Figure 1. The structure of $[Cu_2(IA)_4(DMSO)_2]\cdot CH_3OH$ (**1**) and the atom numbering system (CH_3OH molecules and hydrogens are omitted for clarity).

the atomic numbering system is illustrated in figure 1. The structure consists of two Cu ions linked by four IA^- ligands and two DMSO molecules, which are bound trans to the Cu–Cu vector on each of the Cu ions, similar to those of $[Cu_2(Indo)_4L_2]$ (IndoH = 1-(4-chlorobenzoyl)-5-methoxy-2-methyl-1Hindole-3-acetic acid, L = DMF, N, N-dimethylacetamide (DMA), N-methylpyrrolidone (NMP), dimethyl sulfoxide (DMSO), and water) [10], and the dinuclear structure of $[Cu_2(CH_3COO)_4(H_2O)_2]$ [11]. In the centrosymmetric and binuclear structure, Cu1 and Cu2 are in two different distorted octahedra with four short Cu–O (IA^-) bond lengths (1.965(5)–1.995(5)Å for Cu1 and 1.954(5)–1.982(5)Å for Cu2, and a long solvent Cu–O bond length (2.153(6)Å for Cu1 and 2.168(6) for Cu2. The O–Cu–O bond angles in the complex are different, indicating a distorted pyramid coordination environment and clear Jahn–Teller axial deformations for both Cu ions. The two oxygens (O9 and O10) from DMSO molecules are almost in a straight line with the two center atoms, their torsional angle is 170.5°. The fused and conjugated five- and six-membered rings of each IA^- are close to being coplanar (deviations less than 0.0250 Å). The two coppers in the dimeric unit are connected by a distance of 2.613(11) Å, similar to that found in $[Cu_2(Indo)_4(DMSO)_2]$ [10] (2.632(6) Å) and other Cu carboxylate dimers [12] and only slightly longer than that found in Cu metal (2.56 Å) [13]. The Cu dimer makes no close contacts with other molecules in the lattice and MeOH molecules are loosely held in the lattice.

3.1.2. Crystal structure of 2. The single crystal X-ray diffraction analysis has revealed that **2** crystallizes in the monoclinic system, space group $P2_1/c$. The crystal structure consists of dimeric molecules, and the two cadmium ions bridged by iodides, as shown in figure 2. The complex has an inversion center located at the middle of the dimer. Both

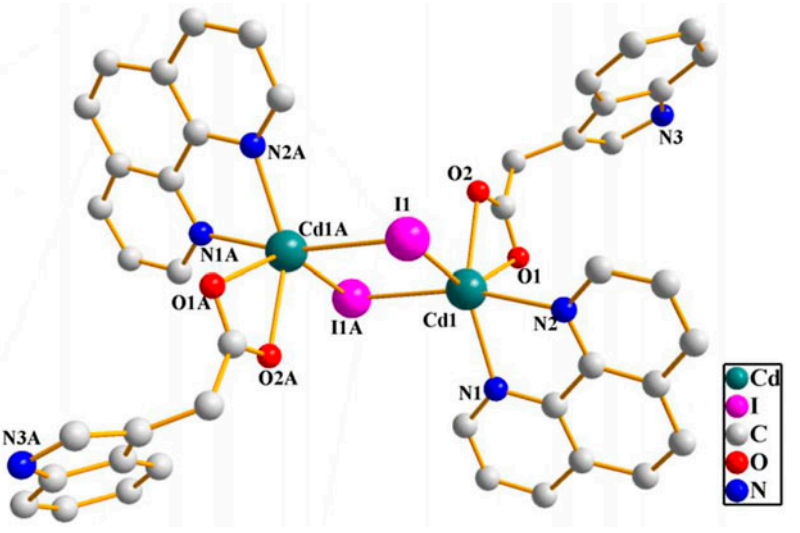

Figure 2. The structure of $[Cd_2(IA)_2(phen)_2I_2]$ (**2**) and the atom numbering system (hydrogens are omitted for clarity).

cadmium ions are six coordinate but with distortion from a regular octahedral arrangement. Each cadmium is located in a seriously distorted octahedron and coordinated to O1 and O2 from one IA^-, two nitrogens (N1, N2) from one phen and two bridged iodides. O1, O2, N1, and I1A are located at equatorial positions with maximum deviation from the best least-squares plane being 2.8000 Å; N2 and I1 are located at two axial sites with N2–Cd1–I1 angle of 165.62. The Cd1–O1 and Cd1–O2 bond distances are 2.491(5) and 2.288(4) Å, respectively, falling within the normal range (2.251–2.879 Å) [14]. In this system, the quadrilateral plane constituted by Cd1, I1, Cd1A, and I1A is completely planar (maximum deviation from the best least-squares plane being 0.0000 Å), with the Cd–I side length of 2.914 Å and the angles of 87.04° and 92.96°. The long Cd···Cd distance (4.013 Å) indicates that there is no interaction between cadmium ions [15]. In addition, there exist hydrogen bonding interactions of N–H···O involving the oxygen and nitrogen from IA ligands, and the distance of N–H···O is 2.124 Å, which is stronger than reported N–H···O hydrogen bonds [16]. The existence of the hydrogen bonds makes the structure more stable.

Complex **2** is different from reported mononuclear $[Cd(phen)(IA)_2]$, which was obtained by assembly of $Cd(OAc)_2$ and IAH, and also crystallizes in the monoclinic system, space group $P2_1/c$ [17]. Considering the two above Cd(II)-phen-HA^- complexes, it is obvious that iodide bridges play an important role in the dimeric Cd(II)-phen-HA^- complex.

3.1.3. Crystal structure of 3. Single X-ray determination shows that **3** crystallizes in the triclinic system, space group *P-1*. As shown in figure 3, **3** presents an interesting 1-D chain based on secondary building units (SBUs) of $[Pb_2(IA)_4]$, which contain two crystallographic independent Pb1 and Pb2 ions. Both lead ions are irregularly six coordinate by six oxygens from four IA^- ligands with slightly different bond lengths and angles. The observed Pb–O bond lengths are of 2.378(8)–2.669(8) Å, typical for such bonds [18]. The bond angles around Pb are between 50.9(3)° and 166.9°. The coordination geometry of Pb1 and Pb2

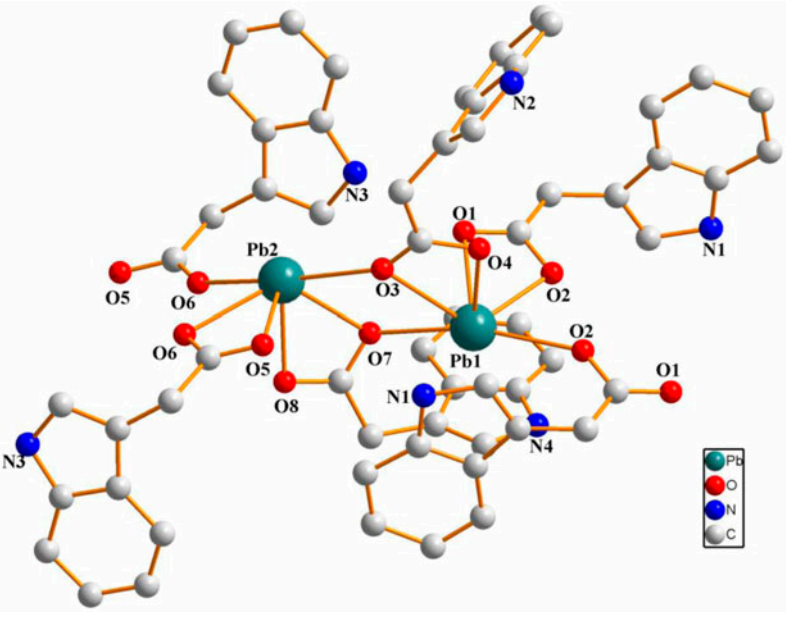

Figure 3. Two types of Pb in $\{[Pb_2(IA)_4]\cdot CH_3OH\}_n$ (**3**) and their atom numbering system (CH_3OH and hydrogens are omitted for clarity).

can be described as half a dodecahedron with two adjacent sites vacant where a lone pair of electrons might be located.

Each carboxylate oxygen is bridged to one Pb ion, as shown in figure 4, the interconnection of the above two types of Pb ions via bridging carboxylates results in a 1-D chain. It can be seen that there are three types of Pb–O–Pb–O rings: Pb1–O2A–Pb1A–O2, Pb1–O3–Pb2–O7, and Pb2–O6–Pb2A–O6A, which are similar to those in the structures of reported Pb-carboxylate polymers [19]. Each ring is bridged by Pb ions and strictly coplanar: the dihedral angles between planes Pb2–O6–Pb2A–O6A (the mean deviation from the plane is 0.0000 Å) and Pb1–O2A–Pb1A–O2 (the mean deviation from the plane is 0.0000 Å), Pb2–O6–Pb2A–O6A and Pb1–O3–Pb2–O7 (the mean deviation from the plane is 0.0111 Å), Pb1–O2A–Pb1A–O2 and Pb1–O3–Pb2–O7 are 26.3°, 118.0°, and 107.3°, respectively. The intrachain distances between metallic cations are 4.220 Å for Pb1···Pb1, 4.344 Å for Pb2···Pb2, and 4.360 Å for Pb1···Pb2. In the solid-state structure, the chains pack through van der Waals interactions.

3.2. *UV absorption spectra*

To further examine the coordination of metal ions with IAH, we determined the UV absorption spectra of the ligand and **1**, **2**, and **3**. Figure 5 shows the absorption spectra of **1**, **2**, and **3** in DMF ($c = 1.0 \times 10^{-5}$ M dm^{-3}) solution. The ligand shows intense absorption in 235 nm and a low energy absorption in 270 nm, from $\pi \rightarrow \pi^*$ transition within IAH. Complexes **1** and **3** have the same absorption as the free ligand, showing that their coordination behaviors do not influence the electronic transition within the ligand. But **2** has a different

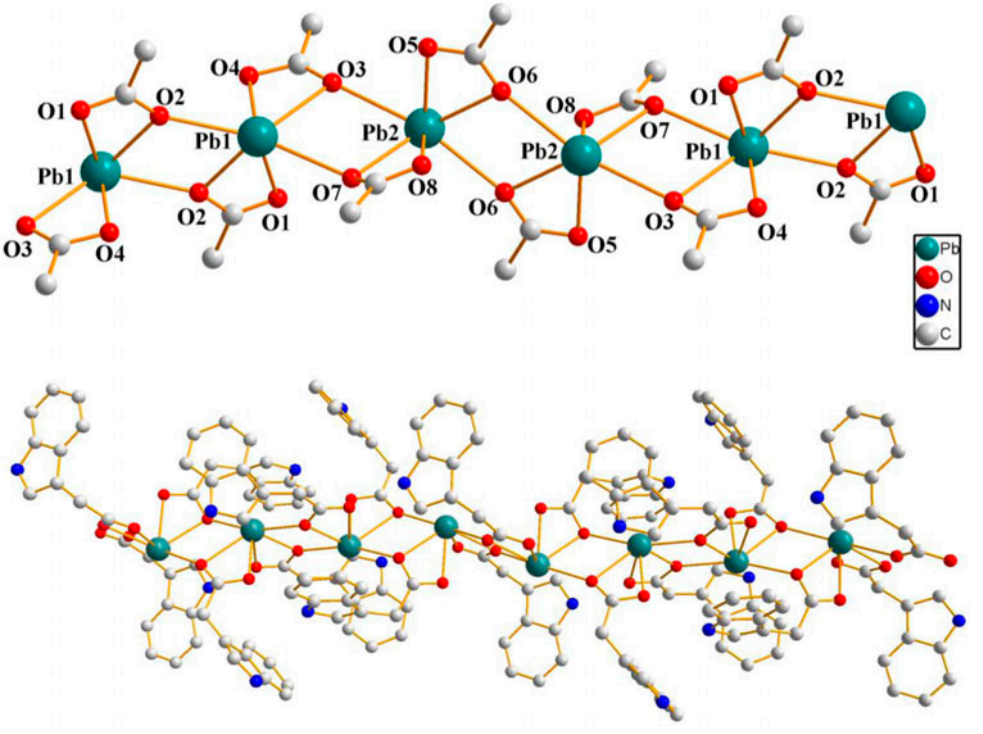

Figure 4. The infinite 1-D chain with atom-labeling scheme of **3**.

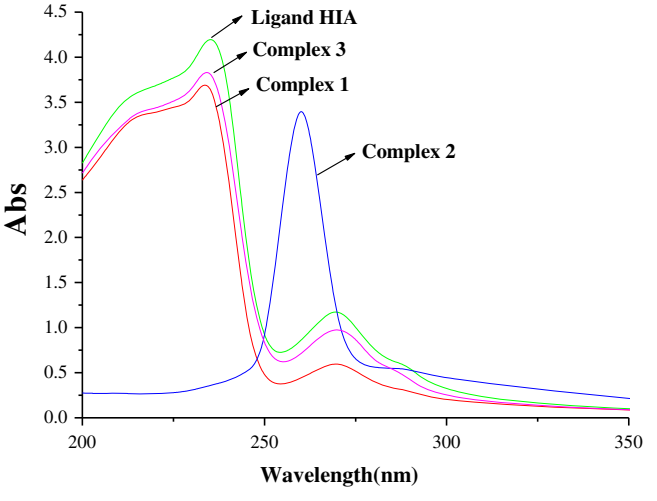

Figure 5. UV–vis absorption spectra in DMF for the ligand, **1**, **2** and **3** with the concentration of 1×10^{-5} M dm^{-3}.

absorption band with only one absorption at 255 nm. This may be due to **2** containing a strong conjugation caused by phen, so that the complex forms a strong delocalization [20].

3.3. *Selective luminescent responses of 2 to various metal ions*

Our previous research reported two fluorescent sensors of zinc(II), $[Zn(IA)_2(phen)]$, and $[Zn(IA)_2(4,4'\text{-bipy})]_n \cdot C_2H_5OH$, which exhibit fluorescence quenching when Hg^{2+} ions are present, showing high selectivity and sensitivity for Hg^{2+} recognition [8]. For our continuing research of metal–indoleacetic complexes for detecting metal ions, we investigated the selective luminescent responses of **1**, **2**, and **3** to various metal ions. In addition, ^1H NMR spectra in deuterated DMSO solution reveal that all the three complexes cause changes in the chemical shifts in comparison with free ligand HIA (figures S1–S4, see online supplemental material at http://dx.doi.org/10.1080/00958972.2014.960404). Some main peaks shift to low fields and the characteristic peak at $\delta = 12.16$ [1H, –COOH] disappear, indicating that carboxyl oxygen from IA^- coordinate to metal ions and the Cu–O, Cd–O, and Pb–O bonds of complexes in DMSO solution have not been cleaved. Thus, the structures of the complexes are maintained in solution for sensing.

Investigation of fluorescence response behaviors showed that **1** and **2** exhibited similar fluorescence emissions in DMF/H_2O mixture solution, giving one emission maximum around 340 ($\lambda_{ex} = 280$ nm) and 345 nm (characteristic for the indole moiety, $\lambda_{ex} = 297$ nm) at room temperature, respectively. Beside a maximum emission around 340 nm, the emission spectrum of **3** has a new emission band located at longer wavelength ($\lambda = 602$ nm) upon photoexcitation at 291 nm. The fluorescent changes of **3** can be attributed to completely different metal cation binding modes [21].

The chemosensor behavior of **1**, **2**, and **3** with different metal ions were investigated by interaction with 1.0×10^{-5} M dm^{-3} of representative alkali (Na^+, K^+), alkaline earth (Mg^{2+}, Ca^{2+}), and transition-metal ions (Mn^{2+}, Cr^{3+}, Fe^{3+}, Ni^{2+}, Cd^{2+}, Co^{2+}, Cu^{2+}, Hg^{2+}, Ag^+) and Pb^{2+}, respectively. The experiment results are shown in figures 6–8. From the figures, the

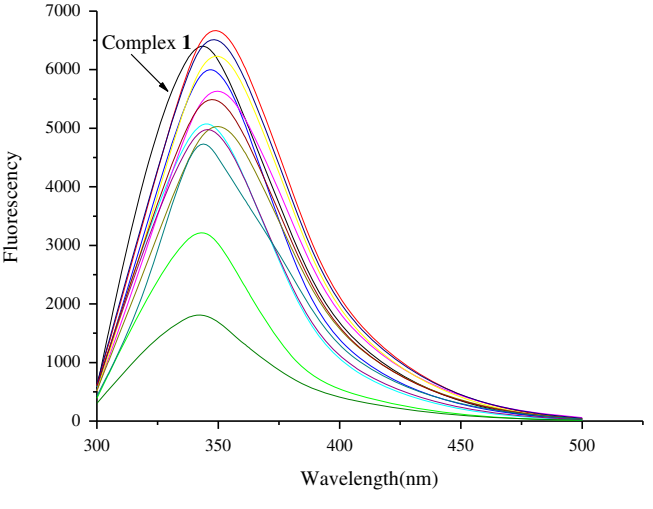

Figure 6. Fluorescence spectra of **1** in response to Na^+, K^+, Mg^{2+}, Ca^{2+}, Mn^{2+}, Cr^{3+}, Fe^{3+}, Ni^{2+}, Cd^{2+}, Co^{2+}, Cu^{2+}, Hg^{2+}, Ag^+, Pb^{2+} ions. $\lambda_{ex} = 280$ nm, **1** = 1.0×10^{-5} M dm^{-3}.

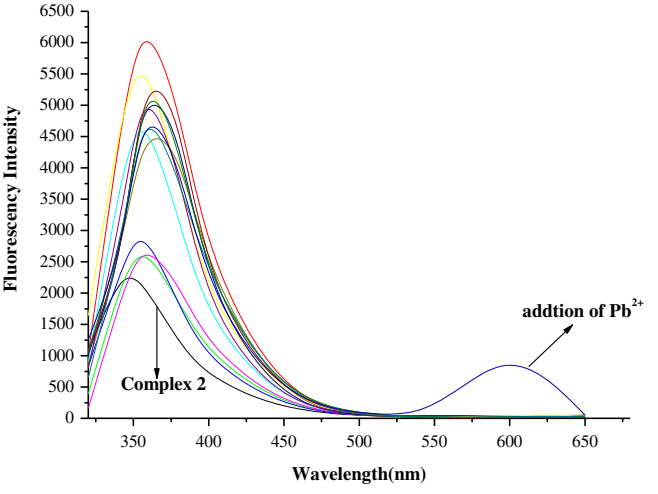

Figure 7. Fluorescence spectra of **2** in response to Na^+, K^+, Mg^{2+}, Ca^{2+}, Mn^{2+}, Cr^{3+}, Fe^{3+}, Ni^{2+}, Cd^{2+}, Co^{2+}, Cu^{2+}, Hg^{2+}, Ag^+, Pb^{2+} ions. λ_{ex} = 297 nm, **2** = 1.0×10^{-5} M dm^{-3}.

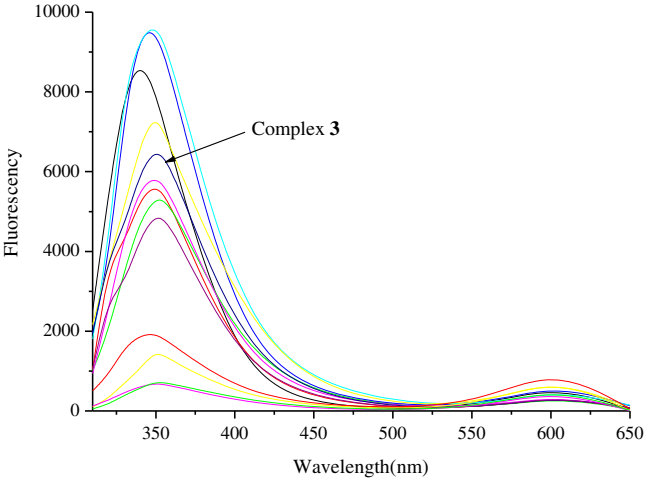

Figure 8. Fluorescence response of **3** to 1.0×10^{-5} M dm^{-3} of Na^+, K^+, Mg^{2+}, Ca^{2+}, Mn^{2+}, Cr^{3+}, Fe^{3+}, Ni^{2+}, Cd^{2+}, Co^{2+}, Cu^{2+}, Hg^{2+}, Ag^+, Pb^{2+} ions in DMF/H_2O (1 : 100 v/v) solution. λ_{ex} = 291 nm, **3** = 1.0×10^{-5} M dm^{-3}.

chemosensor behaviors of **1**, **2**, and **3** towards the metal ions were similar, in which λ_{em} almost kept the same with the free complexes, respectively, only showing slight luminescent intensity change around the maximum emission peak.

Differently, upon addition of Pb^{2+}, the emission spectrum of **2** exhibits excellent fluorescence selectivity towards Pb^{2+} (figure 7), which produces a new maximum emission wavelength at 602 nm, while other metal ions only caused slight luminescent intensity changes around λ_{em} (345 nm). This results in a visually detectable change in solution fluorescence. The profile of this spectral line is the same as that of **3**, suggesting that the fluorescence

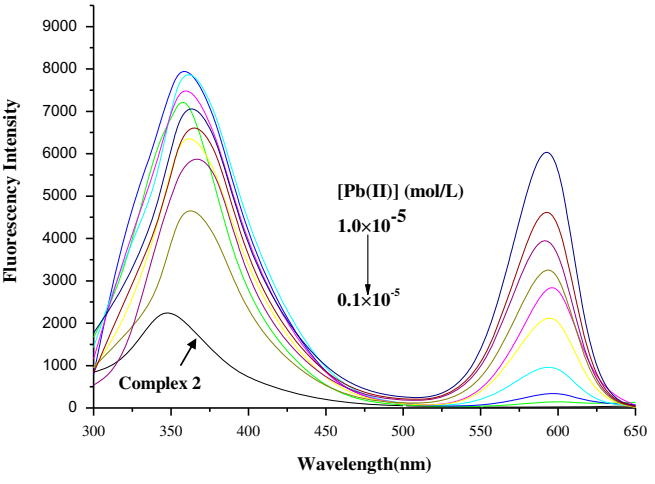

Figure 9. Fluorescence spectra of **2** in DMF/H_2O (1 : 9 v/v) in the presence of increasing concentration of Pb$(NO_3)_2$. λ_{ex} = 291 nm, **2** = 1.0 × 10^{-5} M dm^{-3}.

response of the addition of Pb^{2+} to **2** is the Pb^{2+}-exchanged products of **2**, namely **3**. It is known that PET (photoinduced electron/energy transfer) from the fluorophore to the metal ion is a reasonable explanation [22]. Therefore, interaction of Pb^{2+} with the indole groups induces a fluorescence enhancement and change according to the PET principle. Interestingly, the Pb^{2+}-exchanged products of Zn-HIA complexes can result in fluorescence quench [8], attributed to the electronic charge of the complexes (N and O) transferred to Pb^{2+} (d-orbital) and the electronic charge of the complexes redistributed in an excited state [8, 23].

In order to gain more insight into the chemosensing properties of **2** toward Pb^{2+} ions, a fluorescence titration (figure 9) with $Pb(Ac)_2$ in DMF/H_2O was carried out. Upon the gradual addition of the Pb^{2+} from 0.1 to 1.0 equiv, the new fluorescence band at 600 nm increased steadily. Pb^{2+} could be detected at least down to 1.0 × 10^{-6} M dm^{-3}, a concentration in the ppm range, when **2** was employed at 1.0 × 10^{-5} M dm^{-3}. A very low concentration of Pb^{2+} could induce apparent fluorescence enhancement at longer wavelength (λ = 602 nm).

4. Conclusion

In this work, we report three complexes $[Cu_2(IA)_4(DMSO)_2]\cdot CH_3OH$ (**1**), $[Cd_2(IA)_2(phen)_2I_2]$ (**2**), and $\{[Pb_2(IA)_4]\cdot CH_3OH\}_n$ (**3**) based on the indole-3-acetic acid ligand. The complexes present satisfactory fluorescence emissions, especially for **3**, which exhibits additional near infrared emission at 602 nm. Complex **2** shows highly sensitive and selective sensing to Pb^{2+} by central atom exchange. Compared to recent reported complexes used as sensors for metal cations [24], we have developed a new metal–organic complex based chemosensor for Pb^{2+} detection with high selectivity and sensitivity. The work and our previous work [8] give ideas on the design of chemosensors based on metal–indole acid complexes, which might be a potential luminescent chemosensor for the detection of metal ions. We believe judicious use of metal moieties and modified indole acid ligands are effective routes to obtain highly sensitive and selective methods for detecting metal ions.

Supplementary material

Crystallographic data reported in this paper have been deposited with the Cambridge Crystallographic Data Center as supplementary publication. CCDC numbers are 880369–880371 for **1–3**, respectively. These data can be obtained free of charge via www.ccdc.cam.ac.uk/conts/retrieving.htm (or from the Cambridge Crystallographic Data Center, 12, Union Road, Cambridge CB2 1EZ,UK; fax:+44 1223 336033).

Funding

The authors acknowledge financial support from the National Natural Science Foundation of China [grant number J1210060].

References

[1] (a) Y.J. Cui, Y.F. Yue, G.D. Qian, B.L. Chen. *Chem. Rev.*, **112**, 1126 (2012); (b) Y.Q. Wu, H. Jing, Z.S. Dong, Q. Zhao, H.Z. Wu, F.Y. Li. *Inorg. Chem.*, **50**, 7412 (2011); (c) Z.C. Xu, K.H. Baek, H.N. Kim, J.N. Cui, X.H. Qian, D.R. Spring, I. Shin, J. Yoon. *J. Am. Chem. Soc.*, **132**, 601 (2010); (d) A.W. Czarnik. *Acc. Chem. Res.*, **27**, 302 (1994); (e) J.S. Kim, D.T. Quang. *Chem. Rev.*, **107**, 3780 (2007); (f) Y.P. Cai, X.X. Zhou, Z.Y. Zhou, S.Z. Zhu, P.K. Thallapally, J. Liu. *Inorg. Chem.*, **48**, 6341 (2009); (g) C.J. Liu, J. Ling, X.Q. Zhang, J. Peng, Q.E. Cao, Z.T. Ding. *Anal. Methods*, **5**, 5584 (2013).

[2] (a) B. Zhao, X.Y. Chen, P. Cheng, D.Z. Liao, S.P. Yan, Z.H. Jiang. *J. Am. Chem. Soc. Rev.*, **126**, 15394 (2004); (b) B. Zhao, X.Y. Chen, Z. Chen, W. Shi, P. Cheng, S.P. Yan, D.Z. Liao. *Chem. Commun.*, **21**, 3113 (2009); (c) X.Q. Zhao, B. Zhao, W. Shi, P. Cheng. *CrystEngComm*, **11**, 1261 (2009).

[3] L.R. Yang, S. Song, H.M. Zhang, W. Zhang, Z.W. Bu, T.G. Ren. *Synth. Met.*, **161**, 2230 (2011).

[4] (a)G.B. Li, H.C. Fang, Y.P. Cai, Z.Y. Zhou, P.K. Thallapally, J. Tian. *Inorg. Chem.*, **49**, 7241 (2010); (b) B.C. Tzeng, B.S. Chen, C.K. Chen, Y.P. Chang, W.C. Tzeng, T.Y. Lin, G.H. Lee, P.T. Chou, Y.J. Fu, A.H.H. Chang. *Inorg. Chem.*, **50**, 5379 (2011); (c) H.F. Crouse, J. Potoma, F. Nejrabi, D.L. Snyder, B.T.S. Chohanb, S. Basu. *Dalton Trans.*, **41**, 2720 (2012).

[5] (a) I.A. Bergdhal, M. Vahter, S.A. Counter, A. Schutz, L.H. Buchanan, F. Ortega, G. Laurell, S. Skerfring. *Environ. Res. Sec., A*, **80**, 25 (1999); (b) H.N. Kim, W.X. Ren, J.S. Kim, J. Yoon. *Chem. Soc. Rev.*, **41**, 3210 (2012).

[6] (a) Q.Q. Li, M. Peng, H.Y. Li, C. Zhong, L. Zhang, X.H. Cheng, X.N. Peng, Q.Q. Wang, J.G. Qin, Z. Li. *Org. Lett.*, **14**, 2094 (2012); (b) X.L. Fu, T.T. Lou, Z.P. Chen, M. Lin, W.W. Feng, L.X. Chen. *ACS Appl. Mater. Interfaces*, **4**, 1080 (2012); (c) P. Mahato, S. Saha, E. Suresh, R.D. Liddo, P.P. Parnigotto, M.T. Conconi, M.K. Kesharwani, B. Ganguly, A. Das. *Inorg. Chem.*, **51**, 1769 (2012); (d) S. Saha, P. Mahato, U. Reddy G, E. Suresh, A. Chakrabarty, M. Baidya, S.K. Ghosh, A. Das. *Inorg. Chem.*, **51**, 336 (2012); (e) G.P. Luis, M.M. Quiroz, A.O. Terán, H.S. Ortega, E.M. Valenzuela. *J. Lumin.*, **134**, 729 (2013).

[7] M.Y. Chae, J. Yoon, A.W. Czarnik. *J. Mol. Recognit.*, **9**, 297 (1996).

[8] X.L. Xue, Y.Y. Zhu, B. Xiao, L. Liu, H. Xu. *J. Coord. Chem.*, **64**, 2923 (2011).

[9] G.M. Sheldrick. *SHELX-97, Program for the Solution and Refinement of Crystal Structures*, University of Göttingen, Germany (1997).

[10] J.E. Weder, T.W. Hambley, B.J. Kennedy, P.A. Lay, D. MacLachlan, R. Bramley, C.D. Delfs, K.S. Murray, B. Moubaraki, B. Warwick, J.R. Biffin, H.L. Regtop. *Inorg. Chem.*, **38**, 1736 (1999).

[11] (a) V. Niekerk, J.N. Schoening, F.R.L. *Acta Crystallogr.*, **6**, 227 (1953); (b) P.D. Meester, S.R. Fletcher, A.C. Skapski. *J. Chem. Soc., Dalton Trans.*, 2575 (1973); (c) G.M. Brown, R. Chidambaram. *Acta. Crystallogr., Sect. B*, **29**, 2393 (1973); (d) G. Wilkinson. *Comprehensive Coordination Chemistry. The Synthesis, Reaction, Properties & Application of Coordination Compounds*, Vol. 5, p. 634, Pergamon Press, Oxford (1987).

[12] (a) C.D. Samara, D.P. Kessissoglou, G.E. Manoussakis, D. Mentzafos, A. Terzis. *J. Chem. Soc., Dalton Trans.*, 959 (1990); (b) C. Dendrinou-Samara, P.D. Jannakoudakis, D.P. Kessissoglou, G.E. Manoussakis, D. Mentzafos, A. Terzis. *J. Chem. Soc., Dalton Trans.*, 3259 (1992).

[13] G.H. Aylward, T.J.V. Findlay. *SI Chemical Data*, Wiley, New York (1971).

[14] W. Clegg, J.T. Cressey, A. McCamley, B.P. Straughan. *Acta Crystallogr. Sect. C.*, **51**, 234 (1995).

[15] X.Y. Xu, Z.L. Wang, Q.H. Luo, M.C. Shen, X.G. Zhou, Z.Y. Zhou. *J. Coord. Chem.*, **43**, 281 (1998).

[16] (a) A.C. Cunha, V.F. Ferreira, A.K. Jordão, M.C.B.V.D. Souza, S.M.S.V. Wardell, J.L. Wardell, P.A. Tan, R.P.A. Bettens, S.K. Seth, E.R.T. Tiekink. *CrystEngComm*, **15**, 4917 (2013); (b) H.U. Ung, A.R. Moehlig, S. Khodagholian, G. Berden, J. Oomens, T.H. Morton. *J. Phys. Chem., A*, **117**, 1360 (2013); (c) S.Y. Shi, H.H. Teng, L.M. Chang, Y. Wang, L.N. Xiao, X.B. Cui, J.Q. Xu. *Inorg. Chim. Acta*, **399**, 172 (2013).

[17] Z.F. Chen, L. Huang, H. Liang, R.X. Hu, S.M. Shi, H.K. Fun. *Appl. Organometal. Chem.*, **17**, 879 (2003).
[18] H. Xu, Z.Y. Chao, Y.L. Sang, H.W. Hou, Y.T. Fan. *Inorg. Chem. Commun.*, **11**, 1436 (2008).
[19] (a) X.J. Lei, M.Y. Shang, A. Patil, E.E. Wolf, T.P. Fehlner. *Inorg. Chem.*, **35**, 3217 (1996); (b) M.R.St.J. Foreman, M.J. Plater, J.M.S. Skakle. *J. Chem. Soc., Dalton Trans.*, 1897 (2001); (c) M.R.St.J. Foreman, T. Gelbrich, M.B. Hursthouse, M.J. Plater. *Inorg. Chem. Commun.*, **3**, 234 (2000).
[20] (a) P.S. Braterman, J.I. Song, R.D. Peacock. *Inorg. Chem.*, **31**, 555 (1992); (b) Q.L. Zhang, J.G. Liu, H. Chao, G.Q. Xue, L.N. Ji. *J. Inorg. Biochem.*, **83**, 49 (2001).
[21] K.M.K. Swamy, H.N. Kim, J.H. Soh, Y.M. Kim, S.J. Kima, J.Y. Yoon. *Chem. Commun.*, **14**, 1234 (2009).
[22] B. Valeur, I. Leray. *Coord. Chem. Rev.*, **205**, 3 (2000).
[23] Y. Liu, M. Yu, Y. Chen, N. Zhang. *Bioorg. Med. Chem.*, **17**, 3887 (2009).
[24] (a) X.Y. Cheng, M.F. Wang, Z.Y. Yang, Y. Li, T.R. Li, C.J. Liu, Q.X. Zhou. *J. Coord. Chem.*, **66**, 1847 (2013); (b) J.B. Chao, Y. Zhang, H.F. Wang, Y.B. Zhang, F.J. Huo, C.X. Yin, L.P. Qin, Y. Wang. *J. Coord. Chem.*, **66**, 3857 (2013); (c) X.L. Jin, Z.Y. Yang, T.R. Li, B.D. Wang, Y. Li, M.H. Yan, C.J. Liu, J.M. An. *J. Coord. Chem.*, **66**, 300 (2013); (d) C.J. Liu, Z.Y. Yang, M.H. Yan. *J. Coord. Chem.*, **65**, 3845 (2012); (e) R. Arabahmadi, S. Amani. *J. Coord. Chem.*, **66**, 218 (2013); (f) X. Jia, X.T. Yu, G.L. Zhang, W.S. Liu, W.W. Qin. *J. Coord. Chem.*, **66**, 662 (2013).